Use of Finite Taylor Developments Method to Determine the Flow Coefficient of Small Orifices

PhD. Eng. **Andrei VOINEA**[1], Assoc. Prof. PhD. Eng. **Lucian MÂNDREA**[2], Prof. em. PhD. Eng. **Valeriu PANAITESCU**[3]

[1] University POLITEHNICA of Bucharest, Romania, e-mail: andreilucianvoinea@yahoo.com

[2] mandrea_lucian@hotmail.com

[3] valeriu.panaitescu@yahoo.com

Abstract: *This paper presents the finite Taylor developments method used to integrate the Navier-Stokes equations with the purpose of obtaining the hydrodynamic spectrum of the flow in a tank and also in the orifice contracted section of the liquid exit. The authors created a computing program which allows running also at high Reynolds numbers to determine the theoretical value of the orifice flow coefficient. An experimental installation was also made to obtain the practical value of the flow coefficient. Conclusions were obtained comparing the two values.*

Keywords: *flow coefficient, current lines, orifice, numerical methods.*

1. Introduction

The main objective of the paper is to determine the flow coefficient of an orifice using numerical methods. The authors solve the system of flow equations for different Reynolds numbers, first with Re = 1, then with the values 10 and 1000.
The finite Taylor developments method was used and different flow patterns where obtained, represented with the values of the current function ψ.
In the experimental research the Re number of the flow through circular orifices has been defined with the diameter d of the orifice to determine the variations of the flow coefficient μ,

$$\mathrm{Re} = \frac{d\sqrt{2gH}}{\upsilon} \tag{1}$$

$$\mu = \varphi_c \varphi_v \tag{2}$$

H is the orifice head and *υ* is the kinematic viscosity.
Synthesizing the experimental results, there is obtained a diagram that shows the dependence of the velocity coefficient φ_v, contraction coefficient φ_c, and flow coefficient μ with the Re number [1]. Subsequently the diagram was completed with their variation in laminar flow regime as in figure 1, [2], [3].

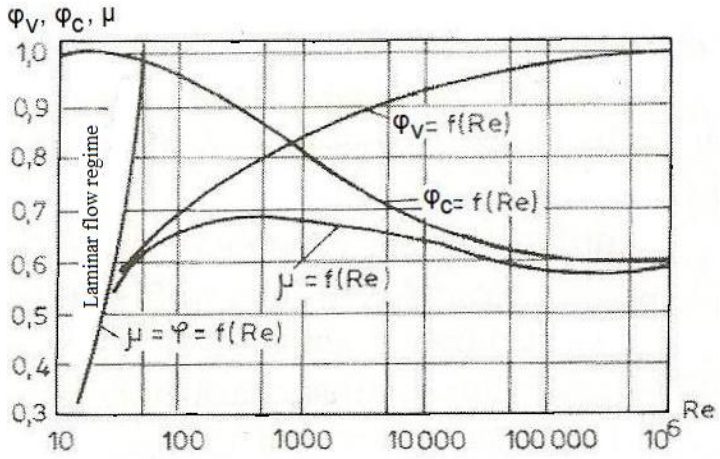

Fig. 1. Dependence of the φ_v, φ_c and μ coefficients according to Re

The μ coefficient dependence on the H head orifice is expressed implicitly by the Reynolds number. The numerical solution obtained can solve the problem of determining the contraction coefficient of an orifice and with the help of this value.
Then the orifice flow coefficient can be determined and finally the actual flow rate which flows out of the tank.

2. The numerical solution of the flow

It is considered a flow through a tank with free surface, fueled at the top and provided with a central orifice at the bottom. The bi-dimensional flow of the fluid is analyzed to estimate the contraction coefficient into the orifice at the bottom of the tank. It is considered that the movement of the liquid phase is permanent, axially symmetric. The dimensionless values are introduced [4], [5], [6], and [7]:

$$r = \frac{R}{R_t},\ z = \frac{Z}{R_t},$$
$$v_r = \frac{V_r}{V_m},\ v_z = \frac{V_z}{V_m}, \tag{3}$$
$$p = \frac{P}{\rho V_m^2},\ \psi = \frac{\Psi}{V_m R_t^2} = \frac{\Psi\pi}{Q},\ \mathrm{Re} = \frac{V_m R_t}{\upsilon}$$

r and z are the dimensionless components of spatial variables, v_r and v_z are the dimensionless velocity components of the horizontal and vertical directions, p the dimensionless pressure, ψ the dimensionless stream function and Re the dimensionless Reynolds number used in the literature to determine the Re number in the tank.
Within formulas R is the radius and Z the share of the vertical point of interest, R_t is the maximum radius of the tank, Z_t maximum height of the tank, V_m the medium velocity, P the pressure, Q is the volumetric flow rate of the liquid and υ is the kinematic viscosity of the liquid.
Using the Reynolds number of the flow inside the tank as well as the previous dimensionless values in the Navier-Stokes equations system, the partial differential equation is obtained [4], [5], [6], and [7]:

$$\psi^{IV}_{r^4} + 2\psi^{IV}_{r^2z^2} + \psi^{IV}_{z^4} - 2\frac{\psi^{III}_{r^3} + \psi^{III}_{rz^2}}{r} + \frac{3}{r^2}\left(\psi^{II}_{r^2} - \frac{\psi^{I}_{r}}{r}\right) =$$
$$\mathrm{Re}\left(\frac{3\psi^{I}_{z}\psi^{I}_{r}}{r^3} + \frac{\psi^{II}_{rz}\psi^{I}_{r} - 2\psi^{II}_{z^2}\psi^{I}_{z} - 3\psi^{II}_{r^2}\psi^{I}_{z}}{r^2} + \frac{\psi^{III}_{r^3}\psi^{I}_{z} - \psi^{III}_{z^3}\psi^{I}_{r} - \psi^{III}_{r^2z}\psi^{I}_{r} + \psi^{III}_{rz^2}\psi^{I}_{z}}{r}\right) \tag{4}$$

It is considered that the velocity is zero on the solid walls.
The next conditions for the stream function were imposed in order to solve the problem, $\Psi = 0$ on the solid wall of the tank.
The flow field is covered by a rectangular network with constant steps,
$\Delta r = h$ and $\Delta z = k$, as in figure 2.

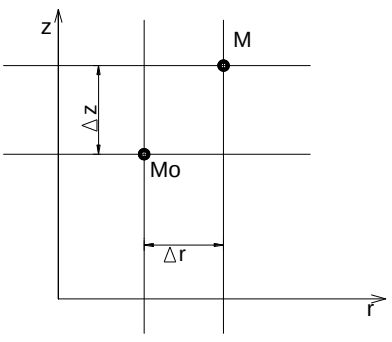

Fig. 2. The steps of the network

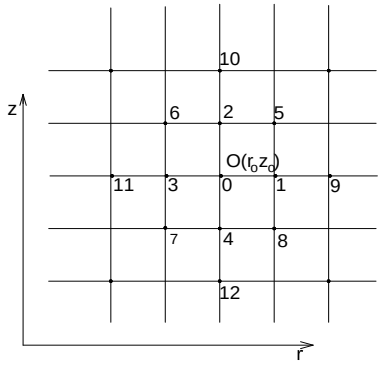

Fig. 3. The network and the nodes numbering

Finite Taylor developments for the current function Ψ were used, and the derivatives of this function up to order IV were obtained, including the values of the current functions in the nodes of the network

$$\psi_r^{I} = \frac{\psi_1 - \psi_3}{2h}; \qquad \psi_z^{I} = \frac{\psi_2 - \psi_4}{2k};$$
$$\psi_{r^2}^{II} = \frac{\psi_1 - 2\psi_0 + \psi_3}{h^2}; \qquad \psi_{z^2}^{II} = \frac{\psi_2 - 2\psi_0 + \psi_4}{k^2};$$
$$\psi_{r^3}^{III} = \frac{\psi_9 - 2\psi_1 + 2\psi_3 - \psi_{11}}{2h^3}; \qquad \psi_{z^3}^{III} = \frac{\psi_{10} - 2\psi_2 + 2\psi_4 - \psi_{12}}{2k^3}; \tag{5}$$
$$\psi_{r^2z}^{III} = \frac{\psi_5 + \psi_6 - \psi_7 - \psi_8 - 2\psi_2 + 2\psi_4}{2h^2k};$$
$$\psi_{r^4}^{IV} = \frac{\psi_9 - 4\psi_1 + 6\psi_0 - 4\psi_3 + \psi_{11}}{h^4};$$
$$\psi_{r^2z^2}^{IV} = \frac{\psi_5 + \psi_6 + \psi_7 + \psi_8 - 2(\psi_1 + \psi_2 + \psi_3 + \psi_4) + 4\psi_0}{h^2k^2}$$

Ψ is the stream function value at the points 1, 2 ... n (nodes) [4], [5], [6], [7]. The relations (5) are replaced in the partial derivatives equation (4).
By distributing the corresponding terms of ψ_0 and Re, algebraic formula associated with partial derivatives equation is obtained

$$\alpha\psi_0 = \beta + \mathrm{Re}\,\delta \tag{6}$$

The coefficients α, β and δ have the expressions:

$$\alpha = 6\left(\frac{1}{h^4} + \frac{1}{k^4} - \frac{1}{r^2h^2}\right) + \frac{8}{h^2k^2} - \mathrm{Re}\left(\frac{3}{h^2} + \frac{2}{k^2}\right)\frac{\psi_2 - \psi_4}{r^2k};$$
$$\beta = \left[4\left(\frac{1}{h^2} + \frac{1}{k^2}\right) - \frac{3}{r^2}\right]\frac{\psi_1 + \psi_3}{h^2} - \left[2\left(\frac{1}{h^2} + \frac{1}{k^2}\right) - \frac{3}{2r^2}\right]\frac{\psi_1 - \psi_3}{rh} +$$
$$+ 4\left(\frac{1}{h^2} + \frac{1}{k^2}\right)\frac{\psi_2 + \psi_4}{k^2} - \frac{\psi_9 + \psi_{11}}{h^4} - \frac{\psi_{10} + \psi_{12}}{k^4} - 2\frac{\psi_5 + \psi_6 + \psi_7 + \psi_8}{h^2k^2} +$$
$$+ \frac{\psi_9 - \psi_{11}}{rh^3} + \frac{\psi_5 - \psi_6 - \psi_7 + \psi_8}{rhk^2}; \tag{7}$$
$$\delta_1 = \frac{\psi_1 - \psi_3}{4hk}\left(3\frac{\psi_2 - \psi_4}{r} - \frac{\psi_{10} - \psi_{12}}{k^2} - \frac{\psi_5 + \psi_6 - \psi_7 - \psi_8}{h^2} + \frac{\psi_5 - \psi_6 + \psi_7 - \psi_8}{2rh}\right);$$
$$\delta_2 = \frac{\psi_2 - \psi_4}{k}\left(\frac{\psi_9 - \psi_{11}}{9h^3} - 3\frac{\psi_1 + \psi_3}{2rh^2} - \frac{\psi_2 + \psi_4}{rk^2} + \frac{\psi_5 - \psi_6 - \psi_7 + \psi_8}{4hk^2}\right)$$
$$\delta = \frac{\delta_1 + \delta_2}{r}$$

h and *k* are the calculating steps on horizontal and vertical directions.
For the points located near the lower horizontal border, according to the reflection principle, $\psi_1 = \psi_0$.
For the lower right corner (figure 4), $\psi_{12} = \psi_0$ and $\psi_9 = \psi_0$, the coefficient *α* has the expression above [4], [5], the rest of the coefficients remains the same.

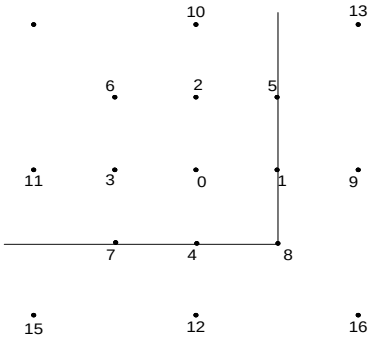

Fig. 4. Points of the network on the down right corner

$$\alpha = 6\left(\frac{1}{h^4}+\frac{1}{k^4}-\frac{1}{r^2h^2}\right)+\frac{8}{h^2k^2}-\mathrm{Re}\left(\frac{3}{h^2}+\frac{2}{k^2}\right)\frac{\psi_2-\psi_4}{r^2k}+\frac{1}{k^2}- \\ -\mathrm{Re}\frac{\psi_1-\psi_3}{4hk^3r}+\frac{1}{h^4}-\frac{1}{h^3r}-\mathrm{Re}\frac{\psi_2-\psi_4}{9h^3kr}; \quad (8)$$

For the points located near the right wall of the tank, also based on the reflection principles, it is deduced that $\psi_9 = \psi_0$; for the points located near the right upper corner of the tank $\psi_9 = \psi_0$ and $\psi_{10} = -\psi_0$.

The values of the current function in the points on the borders were calculated with specific conditions and then within the network, which has not been affected by one of the above conditions.

Calculation was iterative, starting from the left bottom, each time using the values of the current function previously determined.

It is considered that the accuracy is good enough if the difference of two successive values of the stream function of each network point is below ε, which for hydrodynamic flow spectrum obtained was considered equal to 0.001.

3. Calculation example and the results interpretation

Calculation example corresponds to several Reynolds numbers, and the function ψ takes values between 0 and 1. For Re = 1 the flow occurs slowly approximately along the entire length of the tank, with the current lines approximately parallel.

Considering a plane flow and applying the method presented above, there was obtained the flow spectrum for Re = 1, Re = 10 (figure 5), Re = 100 and Re = 1000 (figure 6), results which opens new possibilities to study and solve problems related to the flow coefficient on the orifices.

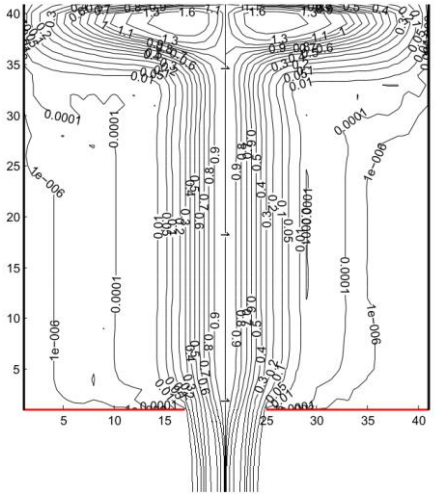

Fig. 5. The current lines for Re = 10

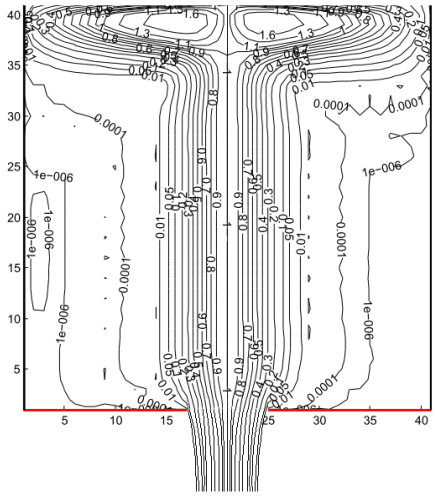

Fig. 6. The current lines for Re = 1000

It is considered that the upper part of the tank is supplied by water dripping and the flow is permanent.
It is determined the contracted section of the fluid jet at different distances from the orifice, namely, at *d*/3, *d*/2, 3*d*/4, and at the length *d*. In literature the maximum contraction considered is at *d*/2 [2] and 0.6*d* [10].
The contraction coefficient φ_c is obtained with the equation

$$\varphi_c = \frac{A_c}{A_g}, \tag{9}$$

A_c is the contracted area of the jet and A_g is the geometric area of the orifice.
The results are shown in Table 1 and inserted in figure 7.

TABLE 1: Dependence of the φ_c coefficient according to Re at different distances from the orifice

Re	1	10	100	1000
–	φ_c			
d/3	0.80210	0.75134	0.73085	0.71318
d/2	0.77951	0.70224	0.65999	0.64835
3*d*/4	0.76353	0.65480	0.58967	0.58752
d	0.76021	0.62853	0.57426	0.56626

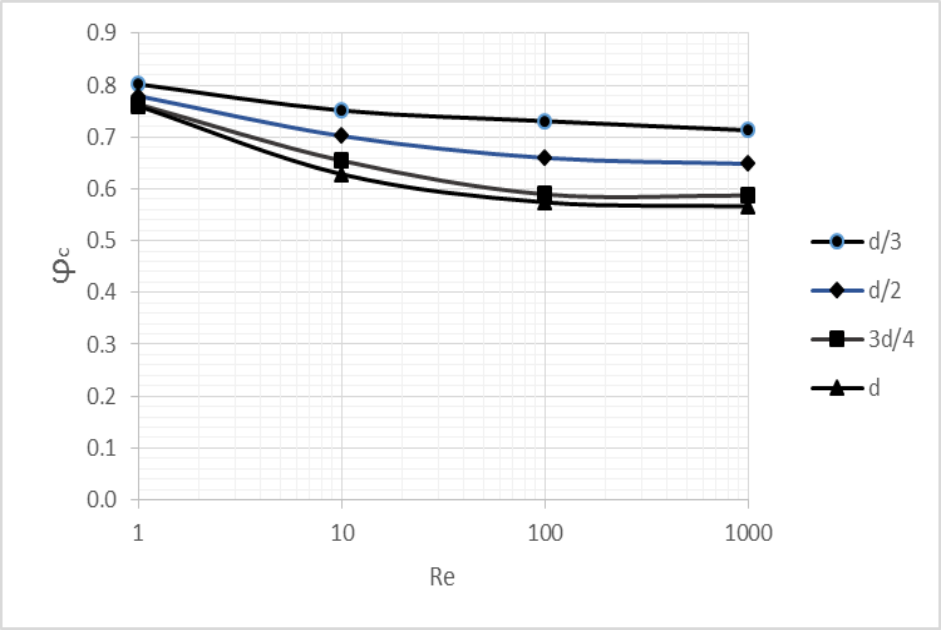

Fig. 7. The contraction coefficients resulted at different contracted areas and at different Re numbers

It is noticed that on the sides of the tank can be found "dead zones" because the liquid flow is concentrated towards the hole. In figure 7, for a better view the Re axis has a logarithmic scale, and it is noticed that the contraction coefficient and implicitly the flow coefficient is influenced by the number Re, decreasing with increasing flow regime.

4. Experimental research

To verify the numerical solution and to study the jet contraction an experimental installation has been designed (fig. 8). It is composed from a cylindrical transparent glass vessel with the inner diameter 187 mm, provided with a circular orifice at the bottom with a diameter *d* = 10 mm, respectively 20 mm.

The cylinder is supplied with water at the top, and to provide a symmetrical flow a vessel with a diameter approximately equal to the glass tank is used.
The vessel has at the bottom orifices equally spaced over the entire surface to ensure equal distribution of the flow over the free surface.
It is maintained a constant level of water H = 200 mm and it is determined the flow rate with the volumetric method.
A flow rate $Q = 1.1 \cdot 10^{-4}$ m^3/s was determined for a permanent flow and the Reynolds number in the tank was Re = 740. Finally, the flow coefficient μ = 0.706 of the circular orifice is determined with the diameter d = 10 mm.
Figure 9 corresponds to the numerical simulation associated with the experimental installation and contains both the flow spectrum in the tank and shape of the liquid jet at the output of the orifice.

Fig. 8. The experimental installation used to determine the flow coefficient.

From the contraction coefficient resulted from simulation φ_c = 0.713, and the velocity coefficient considered in the literature φ_v = 0.97 [11], results the flow coefficient μ = 0.691.
Keeping the same parameters of the experimental installation and by doubling the diameter of the circular orifice d = 20 mm, the flow rate resulted from the measurements is $Q = 0.428 \cdot 10^{-3}$ m^3/s, respectively the Reynolds number in the tank Re = 2850 (fig. 10). The flow coefficient obtained by the ratio resulted from the measured flow divided to the theoretical flow is μ = 0.688.

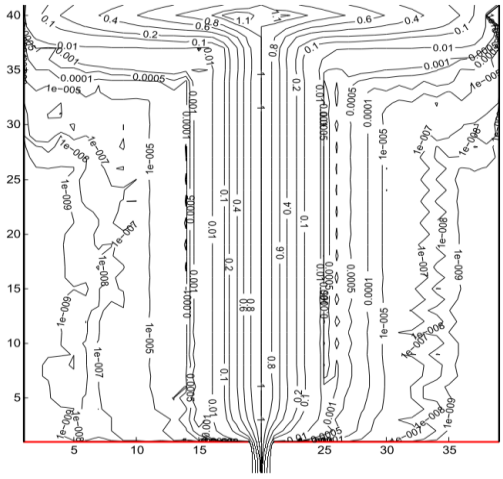

Fig. 9. Current lines for Re = 740, d = 10 mm

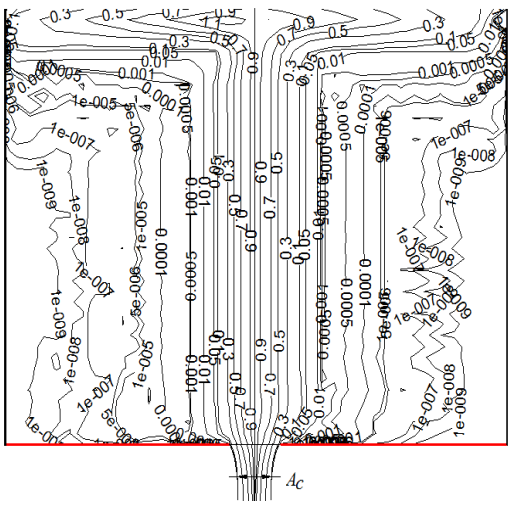

Fig. 10. Current lines for Re = 2900, d = 20 mm

Using the same computing program and changing the diameter of the orifice, a contraction coefficient φ_c = 0.697 is obtained. Multiplying with the velocity coefficient mentioned above, the flow coefficient resulted is μ = 0.676.
For a better visualization of the flow spectrum in the experimental cylindrical tank a colored substance was introduced in the water supply.
The results can be seen in Figure 11, and one can observe that the flow focuses to the center of the tank and at the sides the flow is slow.

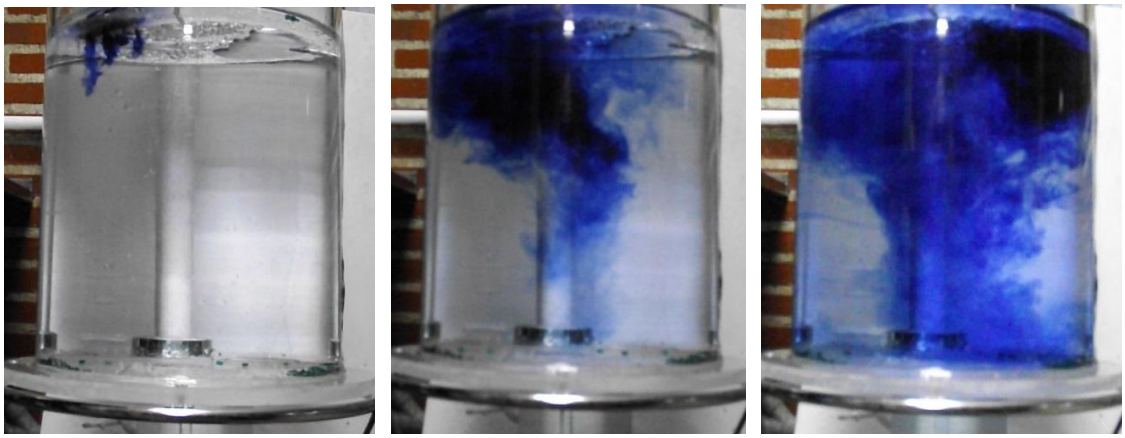

Fig. 11. View of the flow inside the experimental tank

It was obtained an error of −1.5 % for the orifice diameter d = 10 mm, respectively −1.2 % for d = 20 mm, thus it can be concluded that the values determined theoretically are comparable to those obtained experimentally.

5. Conclusions

The numerical solution obtained with the proposed numerical computer program can solve the problem of determining the contraction coefficient of an orifice and with the help of this value it can be determined the flow coefficient of the orifice and finally the actual flow rate which flows out of the tank.
Numerical treatment of the problem allows obtaining the flow spectrum into the tank and indicating areas of vortices, which can facilitate further information to other users.
Due to limited space, the authors could not present all the numerical results, even at higher Reynolds numbers. The authors can only say that the tendency already presented for the contraction coefficients in figure 7 continues.
The experimental installation was made in correspondence with the numerical simulations, and in the end it can be concluded that the values obtained theoretically by the numerical solution are comparable to those obtained experimentally.

References

[1] V. I. Kalitun, E. V. Drozdov, "Osnovî ghidravliki i aerodinamiki". Stroizdat, Moskva 1980, p. 118
[2] S. Hâncu, G. Marin, "Hidraulică teoretică şi aplicată (Theoretical and Applied Hydraulics)", vol. I, Bucharest, 2007, ISBN 978-973-731-476-5, p. 580;
[3] I. E. Idelcik, "Îndrumator pentru calculul rezistenţelor hidraulice (Guide for calculation of hydraulic resistances)", Editura Tehnică, Bucharest, 1984, p. 33;
[4] G. Băran, L. Mândrea, "Studiul curgerii în reactoarele de omogenizare (Study of the flow in homogenizing reactors)". J. Hidrotehnica no. 2, 1998, pp. 39-44;
[5] G. Băran, L. Mândrea, "Influenţa geometriei reactoarelor de omogenizare asupra curgerii (The geometry influence of the homogenizing reactors on the flow)", J. Hidrotehnica no. 8, 1998, pp. 147-149;
[6] G. Băran, L. Mândrea, "Optimizarea formei reactoarelor de omogenizare hidraulică (The shape optimization on hydraulic homogenizing reactors)", J. Hidrotehnica no. 6, 2001, pp.187-190;

[7] L. Mândrea, "Influența formei asupra curgerii în reactoarele de omogenizare (The shape influence on the flow for the homogenizing reactors)", J. Hidrotehnica, no. 4-5, Vol 56, 2011, pp. 33-37;
[8] A. L. Voinea, L. Mândrea, V. Panaitescu. "The determination of an orifice contraction coefficient using numerical methods", 7th International Conference on Energy and Environment CIEM 2015, Iași, October 22 – 23, 2015, CD-ROM, ISSN 2067-0893;
[9] G. Degrez, E. Dick, E. Grundmann, "Course of computational fluid dynamics", Von Karman Institute for Fluid Dynamics, 1992;
[10] C. Mateescu, "Hidraulică (Hydraulics)", Editura Didactică şi Pedagogică, Bucharest, 1963, pp. 471-475;
[11] N. Vasiliu, D. Vasiliu. "Acționări hidraulice şi pneumatice (Hydraulic and pneumatic drives)", vol.1, Bucharest, ISBN 973-31-2248-3, 2005.